Monthly Notices of the ROYAL ASTRONOMICAL SOCIETY

Mon. Not. R. Astron. Soc. **409,** 481–490 (2010) doi:10.1111/j.1365-2966.2010.17329.x

Light curves from rapidly rotating neutron stars

Kazutoshi Numata★† and Umin Lee★

Astronomical Institute, Tohoku University, Sendai, Miyagi 980-8578, Japan

Accepted 2010 July 7. Received 2010 June 27; in original form 2010 April 28

ABSTRACT

We calculate light curves produced by a hotspot of a rapidly rotating neutron star, assuming that the spot is perturbed by a core r mode, which is destabilized by emitting gravitational waves. To calculate light curves, we take account of relativistic effects, such as the Doppler boost due to the rapid rotation and light bending, assuming the Schwarzschild metric around the neutron star. We assume that the core r modes penetrate to the surface fluid ocean to have sufficiently large amplitudes to disturb the spot. For an $l' = m$ core r mode, the oscillation frequency $\omega \approx 2m\Omega/[l'(l'+1)]$ defined in the corotating frame of the star will be detected by a distant observer, where l' and m are, respectively, the spherical harmonic degree and the azimuthal wavenumber of the mode, and Ω is the spin frequency of the star. In a linear theory of oscillation, using a parameter A, we parametrize the mode amplitudes, such that $\max(|\xi_\theta|, |\xi_\phi|)/R = A$ at the surface, where ξ_θ and ξ_ϕ are, respectively, the θ and ϕ components of the displacement vector of the mode and R is the radius of the star. For the $l' = m = 2$ r mode with $\omega = 2\Omega/3$, we find that the fractional Fourier amplitudes at $\omega = 2\Omega/3$ in light curves depend on the angular distance θ_s of the spot centre measured from the rotation axis and become comparable to or even larger than $A \sim 0.001$ for small values of θ_s.

Key words: stars: magnetic field – stars: neutron – stars: oscillations – stars: rotation.

1 INTRODUCTION

Accretion-powered millisecond X-ray pulsars in low-mass X-ray binaries (LMXBs) show small amplitude, almost sinusoidal X-ray time-variations, the dominant periods of which are thought to correspond to the spin periods of the neutron stars (e.g. Lamb & Boutloukos 2008). Lamb et al. (2009) argued that the millisecond X-ray variations are produced by an X-ray-emitting hotspot located at a magnetic pole of the rotating neutron star and that so long as the centre of the hotspot is only slightly off the rotation axis, the X-ray variations produced will have small amplitudes and become almost sinusoidal. They also suggested that if the hotspot is located close to the rotation axis, a slight drift of the hotspot away from the rotation axis leads to appreciable changes in the amplitudes and phases of the X-ray variations. Lamb et al. (2009) pointed out that a temporal change in mass-accretion rates and hence the radius of the magnetosphere, for example, can cause such a drift of the hotspot.

It is now well known that neutron stars can support various kinds of oscillation modes (e.g. McDermott, Van Horn & Hansen 1988). There has been, however, no observational evidence that definitely indicates global oscillations of the stars, probably except for quasi-periodic oscillations (QPOs) observed in the tail of giant X-ray flares from soft gamma-ray repeaters (SGRs) (Duncan 1998; Israel et al. 2005; Strohmayer & Watts 2005, 2006; Watts & Strohmayer 2006), which are believed to have a global magnetic field as strong as $B \gtrsim 10^{14}$ G at the surface (e.g. Woods & Thompson 2006). The QPOs observed in SGRs may be caused by damping oscillations excited when a sudden restructuring of a global magnetic field in the neutron star takes place. For any global oscillations of a neutron star to become observable, mechanisms are needed that excite the oscillations to have amplitudes large enough to produce observable variations in the radiation flux. The ϵ mechanism can be an example of such excitation mechanisms for low-frequency g modes and r modes in the surface fluid layers of mass-accreting neutron stars (e.g. Strohmayer & Lee 1996; Narayan & Cooper 2007). In fact, the r modes propagating in the surface fluid layers of mass-accreting neutron stars have been proposed for the burst oscillations observed during type I X-ray bursts in LMXBs (Strohmayer et al. 1996, 1997; Heyl 2004, 2005; Lee 2004; Lee & Strohmayer 2005). It is also argued that retrograde oscillation modes can be destabilized by emitting gravitational waves, if they satisfy the frequency condition given by $0 < \omega/\Omega < m$ (Friedman & Schutz 1978), and that r modes, which are retrograde modes, become unstable to the gravitational radiation reaction (Andersson 1998), where Ω is the spin

★E-mail: numata@astr.tohoku.ac.jp (KN); lee@astr.tohoku.ac.jp (UL)
†Present address: Hitachi Software Engineering Co. Ltd., Shinagawa, Tokyo 140-0002, Japan.

frequency of the star, ω is the oscillation frequency observed in the corotating frame and m is the azimuthal wavenumber of the mode. r modes in the fluid core of rapidly rotating neutron stars have been a subject of intensive study (e.g. Lindblom, Owen & Morsink 1998; Owen et al. 1998; Lockitch & Friedman 1999; Yoshida & Lee 2000a,b, 2001) and are now regarded as a possible candidate for oscillation modes of a neutron star that are excited to produce observable effects.

If a hotspot on a rapidly rotating neutron star can produce clean light curves without any strong harmonics of the spin frequency, it may be possible to use the light curves as a probe into oscillation modes that are excited to periodically disturb the spot so that the periodicities of the modes manifest themselves in the light curves. In this paper, we calculate light curves by a hotspot taking account of the disturbances by r modes in the fluid core, which are assumed to be excited by emitting gravitational waves. Although the amplitudes of the r modes are confined into the core, in the presence of a global magnetic field, the amplitudes may penetrate to the surface fluid ocean (e.g. Lee 2010). In general, the radial component of the displacement vector of the r modes at the surface has amplitudes much smaller than those of the horizontal and toroidal components, and hence the temperature variations at the surface produced by the r modes would be too small to have observable amplitudes. If the horizontal component of the r modes is large enough to deform the hotspot appreciably, on the other hand, the periodic deformation of the spot may manifest itself in the light curves produced by the hotspot. Section 2 describes the method of solution, numerical results are given in Section 3 and Section 4 provides the conclusion.

2 METHOD OF CALCULATION

We consider a rapidly rotating neutron star having a hotspot on the surface and assume that r modes in the fluid core are destabilized by emitting gravitational waves (Andersson 1998; Friedman & Morsink 1998). For a distant observer, light curves produced by the hotspot will then be observed to have periodic flux variations with the dominant period equal to the spin period of the star. If the core r modes excited by emitting gravitational waves can penetrate the solid crust to have sufficient amplitudes at the surface to give periodic disturbances to the spot, it is expected that the periodicities due to the core r modes will be contained in the light curves from the hotspot. It is the aim of this section to present a method of calculation of light curves produced by a surface hotspot, which is disturbed by a core r mode.

It is convenient to use two Cartesian coordinate systems (x, y, z) and (x', y', z') and to assume that the distant observer is in the x–z and x'–z' planes, where the z-axis is the spin axis of the star and z'-axis is pointing to the distant observer and $y = y'$. We denote the spherical polar coordinates associated with the Cartesian coordinates by (r, θ, ϕ) and (r', θ', ϕ'), where the z-axis (z'-axis) corresponds to the axis defined by $\theta = 0$ ($\theta' = 0$). We denote the inclination angle between the z-axis and z'-axis by i. If we assume Schwarzschild metric to calculate photon trajectories around the spinning neutron star, for a photon emitted from a point (R, θ', ϕ') on the surface of the star and reaching the distant observer, the angle θ' is given by (see Pechenick, Ftaclas & Cohen 1983):

$$\theta' = \int_R^\infty \frac{\mathrm{d}r'}{r'^2}\left[\frac{1}{b^2} - \frac{1}{r'^2}\left(1 - \frac{r_\mathrm{g}}{r'}\right)\right]^{-1/2}, \tag{1}$$

where b is the impact parameter given by

$$b = \frac{R}{\sqrt{1 - r_\mathrm{g}/R}}\sin\delta, \tag{2}$$

where δ is the angle between the surface normal vector $\boldsymbol{n}$ and the direction vector $\boldsymbol{l}$, measured by a non-rotating observer at the stellar surface, of the photon that reaches the distant observer, $r_\mathrm{g} = 2GM/c^2$ is the Schwarzschild radius, R and M are the radius and mass of the star, and G and c are the gravitational constant and the light velocity, respectively. Note that the three vectors $\boldsymbol{n}, \boldsymbol{l}$ and $\boldsymbol{k}'$ are coplanar, where $\boldsymbol{k}'$ is the unit vector along the z'-axis. The observed differential flux d F_E may be given by (e.g. Poutanen & Gierliński 2003):

$$\mathrm{d}F_E = I_E \mathrm{d}O = \frac{\sqrt{1 - r_\mathrm{g}/R}}{D^2}\eta^3 \hat{I}_{\hat{E}}\left(\hat{\delta}\right)\frac{\mathrm{d}\cos\delta}{\mathrm{d}\cos\theta'}\cos\hat{\delta}\,\mathrm{d}\hat{S}, \tag{3}$$

where I_E and dO are the intensity of radiation at energy E and the solid angle seen by a distant observer, respectively, D is the distance to the observer from the centre of the star, $\hat{I}_{\hat{E}}\left(\hat{\delta}\right)$ is the intensity of radiation at energy $\hat{E}$ into the direction angle $\hat{\delta}$ measured from the surface normal and d$\hat{S}$ is the area of a surface element on the surface and the hatted quantities indicate those defined in the frame corotating with the star, and we have used $\cos\delta\ \mathrm{d}S = \cos\hat{\delta}\ \mathrm{d}\hat{S}$ (e.g. Lind & Blandford 1985; Ghisellini 2000). Here, η is the Doppler factor given by

$$\eta = \frac{1}{\gamma\left(1 - \beta\cos\zeta\right)}, \tag{4}$$

where

$$\gamma = \frac{1}{\sqrt{1 - \beta^2}}, \quad \beta = \frac{R\Omega/c}{\sqrt{1 - r_\mathrm{g}/R}}\sin\theta \quad \text{and} \quad \cos\zeta = -\frac{\sin\delta}{\sin\theta'}\sin i\sin\phi. \tag{5}$$

Integrating the flux d F_E by photon energy E measured by a distant observer, we obtain

$$\mathrm{d}F = \frac{(1 - r_\mathrm{g}/R)}{D^2}\eta^5\cos\delta\frac{\mathrm{d}\cos\delta}{\mathrm{d}\cos\theta'}\hat{I}\left(\hat{\delta}\right)\mathrm{d}\hat{S}, \tag{6}$$

where we have used

$$E = \eta\sqrt{1 - r_\mathrm{g}/R}\,\hat{E}, \quad \eta\cos\delta = \cos\hat{\delta} \quad \text{and} \quad \hat{I}\left(\hat{\delta}\right) = \int_0^\infty \hat{I}_{\hat{E}}\left(\hat{\delta}\right)\mathrm{d}\hat{E}. \tag{7}$$

Assuming $\hat{I}(\hat{\delta}) = \hat{I}_0$ is homogeneous blackbody radiation independent of $\hat{\delta}$ and integrating over the surface in the corotating frame, we have

$$F = \left(1 - \frac{r_{\rm g}}{R}\right) \hat{I}_0 \frac{R^2}{D^2} \int_{\hat{S}} \eta^5 \frac{\sin\delta}{\sin\theta'} \frac{{\rm d}\sin\delta}{{\rm d}\theta'} \sin\hat{\theta}\, {\rm d}\hat{\theta}\, {\rm d}\hat{\phi}, \tag{8}$$

where $(\hat{r}, \hat{\theta}, \hat{\phi})$ are spherical polar coordinates in the corotating frame of the star, and we assume $\theta = \hat{\theta}$ and $\phi = \hat{\phi} + \Omega t$ with Ω being the spin frequency of the star observed by a distant observer, and t is the coordinate time at infinity. Hereafter, $(\hat{r}, \hat{\theta}, \hat{\phi})$ and $(\hat{x}, \hat{y}, \hat{z})$ denote coordinates defined in the corotating frame of the star.

To take account of the effects of periodic disturbances due to core r modes on the spot, we first calculate small amplitude oscillations of rotating and magnetized neutron stars in Newtonian dynamics, disregarding general relativistic effects on the oscillations (Lee 2010). We introduce a dipole magnetic field given by $\boldsymbol{B} = \mu_{\rm m}\nabla(\cos\theta/r^2)$, whose magnetic axis is assumed to align with the spin axis of the star, where $\mu_{\rm m}$ is the magnetic dipole moment. Since the magnetic pressure in the deep interior is much smaller than the gas pressure for neutron stars with a magnetic field whose strength at the surface is comparable to or less than $\sim 10^{12}$G, we treat the fluid core as being non-magnetic (e.g. Lee 2007, 2010). Since we have assumed that the spin axis is the magnetic axis, the temporal and azimuthal angular dependence of oscillations can be represented by a single factor ${\rm e}^{{\rm i}(m\hat{\phi}+\omega t)}$, where m is the azimuthal wavenumber around the rotation axis and $\omega \equiv \sigma + m\Omega$ is the oscillation frequency in the corotating frame of the star with σ being the oscillation frequency in an inertial frame. Since the angular dependence of the oscillations in a rotating and magnetized star cannot be represented by a single spherical harmonic function, we expand the perturbed quantities in terms of spherical harmonic functions $Y_l^m(\theta, \phi)$ with different values of l for a given m, considering that the axis of rotation coincides with that of the magnetic field. The displacement vector $\boldsymbol{\xi}$ is then represented by a finite-series expansion of length $j_{\rm max}$ as

$$\frac{\boldsymbol{\xi}}{\hat{r}} = \sum_{j=1}^{j_{\rm max}} \left[S_{l_j}(\hat{r}) Y_{l_j}^m(\hat{\theta}, \hat{\phi}) \hat{\boldsymbol{e}}_r + H_{l_j}(\hat{r}) \nabla_{\rm H} Y_{l_j}^m(\hat{\theta}, \hat{\phi}) + T_{l'_j}(\hat{r})\, \hat{\boldsymbol{e}}_r \times \nabla_{\rm H} Y_{l'_j}^m(\hat{\theta}, \hat{\phi}) \right] {\rm e}^{{\rm i}\omega t}, \tag{9}$$

where $\hat{\boldsymbol{e}}_r$, $\hat{\boldsymbol{e}}_\theta$ and $\hat{\boldsymbol{e}}_\phi$ are the orthonormal vectors in the $\hat{r}$, $\hat{\theta}$ and $\hat{\phi}$ directions, respectively, and

$$\nabla_{\rm H} = \hat{\boldsymbol{e}}_\theta \frac{\partial}{\partial\hat{\theta}} + \hat{\boldsymbol{e}}_\phi \frac{1}{\sin\hat{\theta}} \frac{\partial}{\partial\hat{\phi}}, \tag{10}$$

and $l_j = |m| + 2(j-1)$ and $l'_j = l_j + 1$ for even modes, and $l_j = |m| + 2j - 1$ and $l'_j = l_j - 1$ for odd modes, where $j = 1, 2, 3, \cdots, j_{\rm max}$. Substituting these expansions into the linearized basic equations, we obtain a finite set of coupled linear ordinary differential equations for the expansion coefficients S_{l_j}, H_{l_j} and $T_{l'_j}$ (e.g. Lee 2007, 2010). When the angular dependence of the displacement vector at the surface is represented by the functions $\Xi_j\left(\hat{\theta}\right)$ defined by

$$\Xi_r(\hat{\theta}){\rm e}^{{\rm i}m\hat{\phi}} = \sum_{j=1}^{j_{\rm max}} S_{l_j}(R)\, Y_{l_j}^m(\hat{\theta}, \hat{\phi}) \tag{11}$$

$$\Xi_\theta(\hat{\theta}){\rm e}^{{\rm i}m\hat{\phi}} = \hat{\boldsymbol{e}}_\theta \cdot \sum_{j=1}^{j_{\rm max}} \left[H_{l_j}(R) \nabla_{\rm H} Y_{l_j}^m(\hat{\theta}, \hat{\phi}) + T_{l'_j}(R)\, \hat{\boldsymbol{e}}_r \times \nabla_{\rm H} Y_{l'_j}^m(\hat{\theta}, \hat{\phi}) \right], \tag{12}$$

$$\Xi_\phi(\hat{\theta}){\rm e}^{{\rm i}m\hat{\phi}} = -{\rm i}\hat{\boldsymbol{e}}_\phi \cdot \sum_{j=1}^{j_{\rm max}} \left[H_{l_j}(R) \nabla_{\rm H} Y_{l_j}^m(\hat{\theta}, \hat{\phi}) + T_{l'_j}(R)\, \hat{\boldsymbol{e}}_r \times \nabla_{\rm H} Y_{l'_j}^m(\hat{\theta}, \hat{\phi}) \right], \tag{13}$$

we can rewrite the displacement vector at the surface as

$$\frac{\boldsymbol{\xi}}{R} = \left[\Xi_r(\hat{\theta}) \hat{\boldsymbol{e}}_r + \Xi_\theta(\hat{\theta}) \hat{\boldsymbol{e}}_\theta + {\rm i}\Xi_\phi(\hat{\theta}) \hat{\boldsymbol{e}}_\phi \right] \exp {\rm i}(m\hat{\phi} + \omega t), \tag{14}$$

the real part of which is given by

$$\frac{{\rm Re}\,(\boldsymbol{\xi})}{R} = \left[\Xi_r(\hat{\theta}) \hat{\boldsymbol{e}}_r + \Xi_\theta(\hat{\theta}) \hat{\boldsymbol{e}}_\theta \right] \cos(m\hat{\phi} + \omega t) - \Xi_\phi(\hat{\theta}) \hat{\boldsymbol{e}}_\phi \sin(m\hat{\phi} + \omega t). \tag{15}$$

Note that $m\hat{\phi} + \omega t = m\phi + \sigma t$. In Fig. 1, the functions Ξ_r, Ξ_θ and Ξ_ϕ of the $l' = m = 2$ core r mode calculated for a 0.5-$M_\odot$ neutron star model composed of a fluid core, a solid crust and a fluid ocean are plotted from the left-hand to right-hand panels, for $\bar{\Omega} \equiv \Omega/\sqrt{GM/R^3} = 0.1$, 0.2 and 0.3, where we have assumed $B_0 = 10^{10}$ G with B_0 being the strength of a dipole magnetic field at the surface (see Lee 2010), and in each panel the amplitudes of the functions are normalized by $\max(|\Xi_r|, |\Xi_\theta|, |\Xi_\phi|)$. As shown by the figure, since the amplitudes of the function Ξ_r at the surface are much smaller than those of Ξ_θ and Ξ_ϕ for the r modes, we neglect the term Ξ_r in the following. In a linear theory of stellar oscillations, the amplitudes of the oscillations are indeterminate, and we have to treat the amplitudes as a parameter. In this paper, using a parameter A, we normalize the oscillation amplitudes, such that $\max(|\Xi_\theta(\hat{\theta})|, |\Xi_\phi(\hat{\theta})|) = A$ in $0 \le \hat{\theta} \le \pi$.

Let us write the vector pointing from the stellar centre to the centre of a circular hotspot in the corotating frame as $\hat{\boldsymbol{r}}_{\rm s} = R\hat{\boldsymbol{n}}_{\rm s}$, where

$$\hat{\boldsymbol{n}}_{\rm s} = \sin\hat{\theta}_{\rm s} \cos\hat{\phi}_{\rm s} \hat{\boldsymbol{i}} + \sin\hat{\theta}_{\rm s} \sin\hat{\phi}_{\rm s} \hat{\boldsymbol{j}} + \cos\hat{\theta}_{\rm s} \hat{\boldsymbol{k}}, \tag{16}$$

and $\hat{\theta}_{\rm s}$ denotes the colatitude of the spot centre measured from the spin axis of the star, and $\hat{\boldsymbol{i}}$, $\hat{\boldsymbol{j}}$ and $\hat{\boldsymbol{k}}$ are the orthonormal vectors in the $\hat{x}$, $\hat{y}$ and $\hat{z}$ directions, respectively. If the angular radius of the circular hotspot is equal to α, we have for points $\hat{\boldsymbol{r}} = R\hat{\boldsymbol{n}}$ on the spot

$$\hat{\boldsymbol{n}}_{\rm s} \cdot \hat{\boldsymbol{n}} \ge \cos\alpha, \tag{17}$$

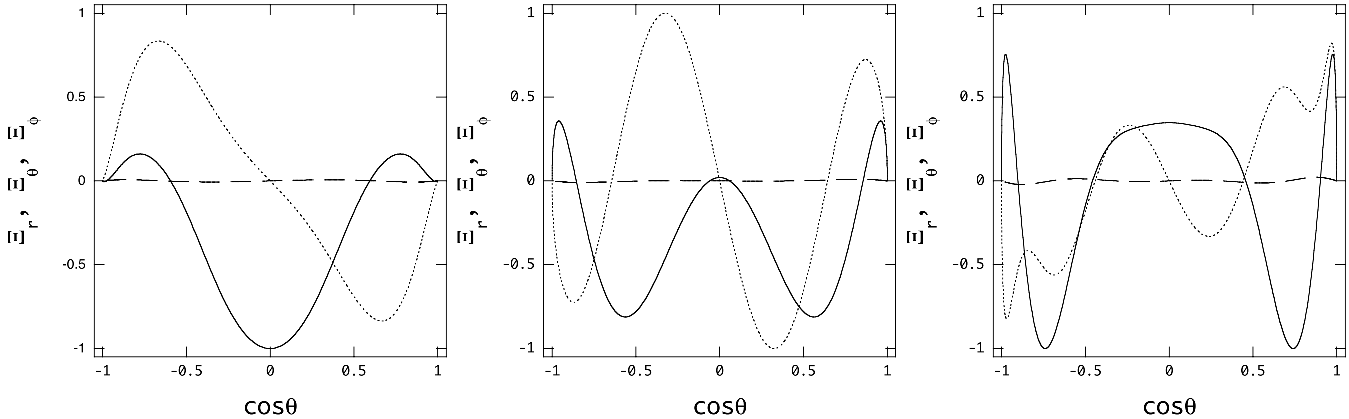

Figure 1. Ξ_r, Ξ_θ and Ξ_ϕ versus $\cos\theta$ for the $l' = m = 2$ r modes calculated for a neutron star model composed of a fluid core, a solid crust and a fluid ocean. The dashed, solid and dotted curves represent Ξ_r, Ξ_θ and Ξ_ϕ, respectively, and the amplitudes are normalized by $\max(|\Xi_r|, |\Xi_\theta|, |\Xi_\phi|)$. For the left-hand, middle and right-hand panels, $\bar\Omega \equiv \Omega/\sqrt{GM/R^3} = 0.1$, 0.2 and 0.3, respectively.

where $\hat{\boldsymbol{n}} = \sin\hat\theta\cos\hat\phi\hat{\boldsymbol{i}} + \sin\hat\theta\sin\hat\phi\hat{\boldsymbol{j}} + \cos\hat\theta\hat{\boldsymbol{k}}$. The outer boundary of the circular spot is given by $\hat{\boldsymbol{n}}_{\rm s}\cdot\hat{\boldsymbol{n}}_{\rm b} = \cos\alpha$, that is,

$$\sin\hat\theta_{\rm b}\sin\hat\theta_{\rm s}\cos(\hat\phi_{\rm b} - \hat\phi_{\rm s}) + \cos\hat\theta_{\rm b}\cos\hat\theta_{\rm s} = \cos\alpha, \tag{18}$$

where $\hat{\boldsymbol{n}}_{\rm b} = \sin\hat\theta_{\rm b}\cos\hat\phi_{\rm b}\hat{\boldsymbol{i}} + \sin\hat\theta_{\rm b}\sin\hat\phi_{\rm b}\hat{\boldsymbol{j}} + \cos\hat\theta_{\rm b}\hat{\boldsymbol{k}}$. If the hotspot is deformed by an r mode having the displacement vector $\boldsymbol{\xi}$, the outer boundary of the spot is approximately given by

$$(\hat r_{\rm d}, \hat\theta_{\rm d}, \hat\phi_{\rm d}) = (R, \hat\theta_{\rm b} + \delta\theta, \hat\phi_{\rm b} + \delta\phi), \tag{19}$$

where

$$\delta\theta = \xi_\theta(R, \hat\theta_{\rm b}, \hat\phi_{\rm b})/R = \Xi_\theta(\hat\theta_{\rm b})\cos(m\hat\phi_{\rm b} + \omega t) \tag{20}$$

and

$$\delta\phi = \xi_\phi(R, \hat\theta_{\rm b}, \hat\phi_{\rm b})/(R\sin\hat\theta_{\rm b}) = -\Xi_\phi(\hat\theta_{\rm b})\sin(m\hat\phi_{\rm b} + \omega t)/\sin\hat\theta_{\rm b}, \tag{21}$$

where $|\boldsymbol{\xi}/R| \ll 1$ is assumed.

If using $\hat{\boldsymbol{n}}$ we define a vector $\hat{\boldsymbol{n}}_\perp$, perpendicular to $\hat{\boldsymbol{n}}_{\rm s}$, as

$$\hat{\boldsymbol{n}}_\perp = \hat{\boldsymbol{n}} - (\hat{\boldsymbol{n}}\cdot\hat{\boldsymbol{n}}_{\rm s})\hat{\boldsymbol{n}}_{\rm s} \equiv -Y\hat{\boldsymbol{e}}^{\rm s}_\theta + X\hat{\boldsymbol{e}}^{\rm s}_\phi, \tag{22}$$

we have

$$X = \sin\hat\theta\sin(\hat\phi - \hat\phi_{\rm s}), \quad Y = -\cos\hat\theta_{\rm s}\sin\hat\theta\cos(\hat\phi - \hat\phi_{\rm s}) + \sin\hat\theta_{\rm s}\cos\hat\theta, \tag{23}$$

where $\hat{\boldsymbol{e}}^{\rm s}_\theta$ and $\hat{\boldsymbol{e}}^{\rm s}_\phi$ are the orthonormal vectors in the $\hat\theta$ and $\hat\phi$ directions and are perpendicular to $\hat{\boldsymbol{e}}^{\rm s}_r = \hat{\boldsymbol{n}}_{\rm s}$. For $\hat{\boldsymbol{n}} = \hat{\boldsymbol{n}}_{\rm b}$ that satisfies equation (18), we obtain

$$X_{\rm b}^2 + Y_{\rm b}^2 = 1 - \cos^2\alpha, \tag{24}$$

where

$$X_{\rm b} = \sin\hat\theta_{\rm b}\sin(\hat\phi_{\rm b} - \hat\phi_{\rm s}), \quad Y_{\rm b} = -\cos\hat\theta_{\rm s}\sin\hat\theta_{\rm b}\cos(\hat\phi_{\rm b} - \hat\phi_{\rm s}) + \sin\hat\theta_{\rm s}\cos\hat\theta_{\rm b}. \tag{25}$$

For $\hat{\boldsymbol{n}} = \hat{\boldsymbol{n}}_{\rm d}$, on the other hand, we have

$$X_{\rm d} = \sin(\hat\theta_{\rm b} + \delta\theta)\sin(\hat\phi_{\rm b} + \delta\phi - \hat\phi_{\rm s}), \quad Y_{\rm d} = -\cos\hat\theta_{\rm s}\sin(\hat\theta_{\rm b} + \delta\theta)\cos(\hat\phi_{\rm b} + \delta\phi - \hat\phi_{\rm s}) + \sin\hat\theta_{\rm s}\cos(\hat\theta_{\rm b} + \delta\phi). \tag{26}$$

A plot of $(X_{\rm d}, Y_{\rm d})$ in a plane may be regarded as a projection of the outer boundary of the deformed spot on to a plane perpendicular to the vector $\hat{\boldsymbol{n}}_{\rm s}$. Examples of the plots $(X_{\rm b}, Y_{\rm b})$ and $(X_{\rm b}, Y_{\rm b})$ are given in Fig. 2 for $\bar\Omega = 0.1$ and in Fig. 3 for $\bar\Omega = 0.3$, where for the spot of $\alpha = 20^\circ$, we have assumed $\theta_{\rm s} = 10^\circ$, 20° and 30°, from the left-hand to right-hand panels in each figure, and $A = 0.1$ for the amplitudes of the functions Ξ_θ and Ξ_ϕ of the $l' = m = 2$ r modes given in Fig. 1. Note that we have assumed for simplicity that the oscillation frequency of the $l' = m = 2$ r mode is exactly equal to $\omega = 2m\Omega/[l'(l'+1)] = 2\Omega/3$ in the corotating frame. The deviation of the r mode frequency from the analytic formula $2m\Omega/[l'(l'+1)]$ for neutron stars depends on various parameters, such as the spin frequency, the solid crust thickness, the equation of state, the thermal stratification in the core, the general relativistic effects, etc., and since it is not our main concern here to investigate how the light curves depend on the frequency deviation, we have simply assumed $\omega = 2m\Omega/[l'(l'+1)]$ for the modes. The figures show periodic deformation of the spot shape, caused by the $l' = m = 2$ r mode, as seen in the corotating frame of the star. As shown by the middle panels of the figures, for $\alpha = 20^\circ$ and $\theta_{\rm s} = 20^\circ$, the outer boundary of the spot touches the pole of $\hat\theta = 0$, at which Ξ_θ and Ξ_ϕ vanish. Since the amplitudes of the functions Ξ_θ and Ξ_ϕ show a sharp increase around the poles for $\bar\Omega = 0.3$, the outer boundary of the spot is largely deformed when $\theta_{\rm s} \sim \alpha$.

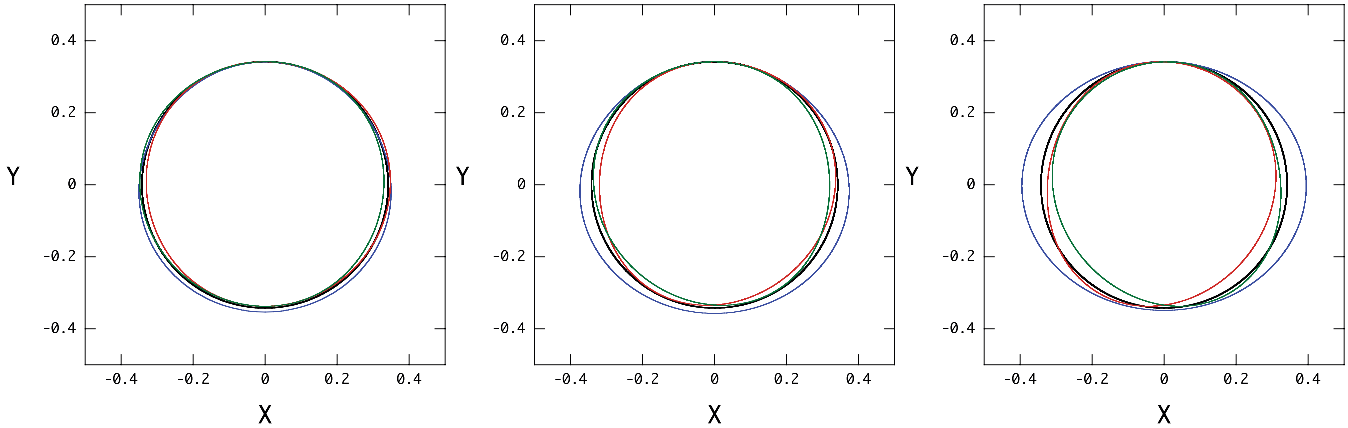

Figure 2. Plots of (X_b, Y_b) and (X_d, Y_d) for the spot of $\alpha = 20°$ computed using the functions Ξ_θ and Ξ_ϕ for the $l' = m = 2$ r mode at $\bar{\Omega} = 0.1$, where $\theta_s = 10°$, $20°$ and $30°$, from the left-hand to right-hand panels, and we assume $\omega = 2\Omega/3$ and $A = 0.1$. Here, the black curve is for the non-perturbed spot (X_b, Y_b) and the blue, red and green curves represent the perturbed spot (X_d, Y_d) at $\Omega t/(2\pi) = 0,\ 1$ and 2, respectively.

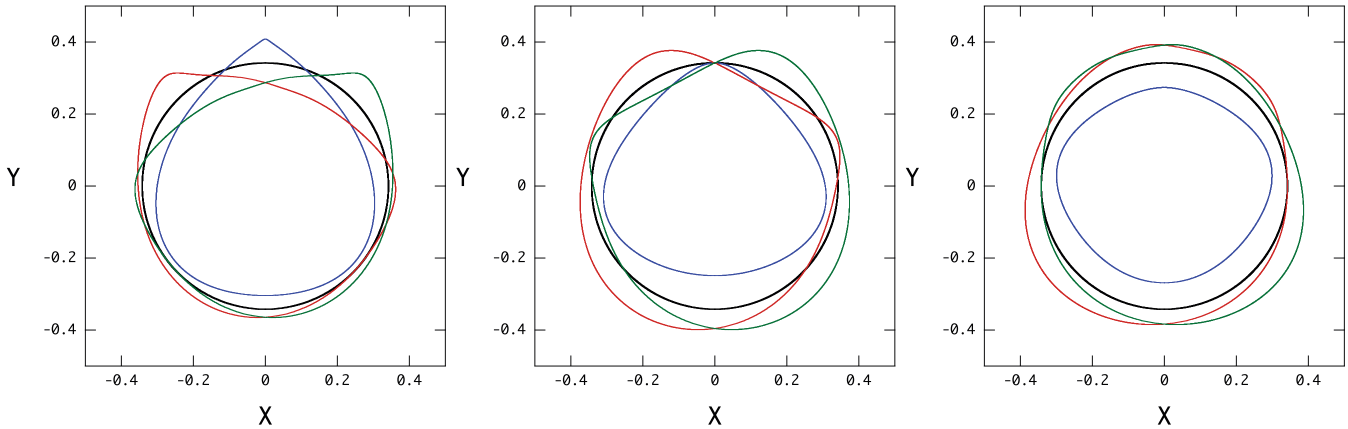

Figure 3. Same as Fig. 2, but for $\bar{\Omega} = 0.3$.

3 NUMERICAL RESULTS

Examples of light curves produced by a hotspot of $\alpha = 20°$ are plotted as a function of $\Omega t/(2\pi)$ in Fig. 4 for $\bar{\Omega} = 0.1$ and in Fig. 5 for $\bar{\Omega} = 0.3$, where $\theta_s = 10°$ for panel (a) and 30° for panel (b), and we have assumed $M = 1.4\,\mathrm{M}_\odot$, $R = 10^6$ cm for the neutron star, and $\omega = 2\Omega/3$ and $A = 0.01$ for the $l' = m = 2$ r modes. Here, we have also assumed that $\hat{I}_0$ is constant. The figures show that the amplitudes of $\delta F = (F - F_m)/F_m$, where F_m is the mean flux, increase when the angular distance θ_s of the spot centre or the inclination angle i increases. An increase in the spin frequency also tends to increase the amplitudes of the variations δF through the Doppler factor, particularly for large values of θ_s and i. For a oscillation amplitude $A = 0.01$, we can clearly see the r modes cause periodic modulations of the amplitudes of δF.

Using light curves $F(t)$, we calculate the discrete Fourier transform $a_j (j = -N/2, \cdots, N/2-1)$ defined by

$$a_j = \sum_{k=0}^{N-1} F(t_k) \exp(2\pi \mathrm{i} f_j t_k), \tag{27}$$

where N is the total number of sampling points in the time-span ΔT, $t_k = k\Delta T/N$, $f_j = j/\Delta T$ and $|a_j| = |a_{-j}|$ for a real function $F(t)$, and k and j are integers. For light-curve calculations, we use $N = N_1 N_2$ with $N_1 = 2^6$ and $N_2 = 2^5$, so that we have the Nyquist frequency $\nu_{\mathrm{Ny}} = 1/(2\delta t)$ with $\delta t = P_s/N_1$ and the time-span $\Delta T = P_s N_2$, where $P_s = 2\pi/\Omega$ is the spin period. In Fig. 6, the fractional Fourier amplitudes a_j/a_0, which are proportional to the fractional rms, are plotted as functions of σ_j/Ω with $\sigma_j \equiv 2\pi f_j$ for light curves calculated assuming $M = 1.4\,\mathrm{M}_\odot$, $R = 10^6$ cm and $\bar{\Omega} = 0.3$. The dominant peak of a_j/a_0 appears at $\sigma_j = \Omega$ due to the spin frequency Ω of the star, which we may call the fundamental, and there also appear weaker peaks at $\sigma_j = 2\Omega$ (first overtone) and 3Ω (second overtone). Because of the periodic modulations caused by the $l' = m = 2$ r mode having the frequency $\omega = 2m\Omega/[l'(l'+1)] = 2\Omega/3$ in the corotating frame, we also have a noticeable peak at $\sigma_j = 2\Omega/3$. Note that a distant observer will detect the r mode frequency measured in the corotating frame, instead of that in an inertial frame, because we are seeing waves restricted to the spot comoving with the star. Although the peak at $\sigma_j = 2\Omega/3$ is almost insensitive to the inclination angle i, the peak at $\sigma_j = \Omega$ becomes higher as i or θ_s increases (e.g. Lamb et al. 2009). It is reasonable that the peak at $\sigma_j = 2\Omega/3$ is approximately proportional to the amplitude parameter A, but the peak at $\sigma_j = \Omega$ is insensitive to it. We also

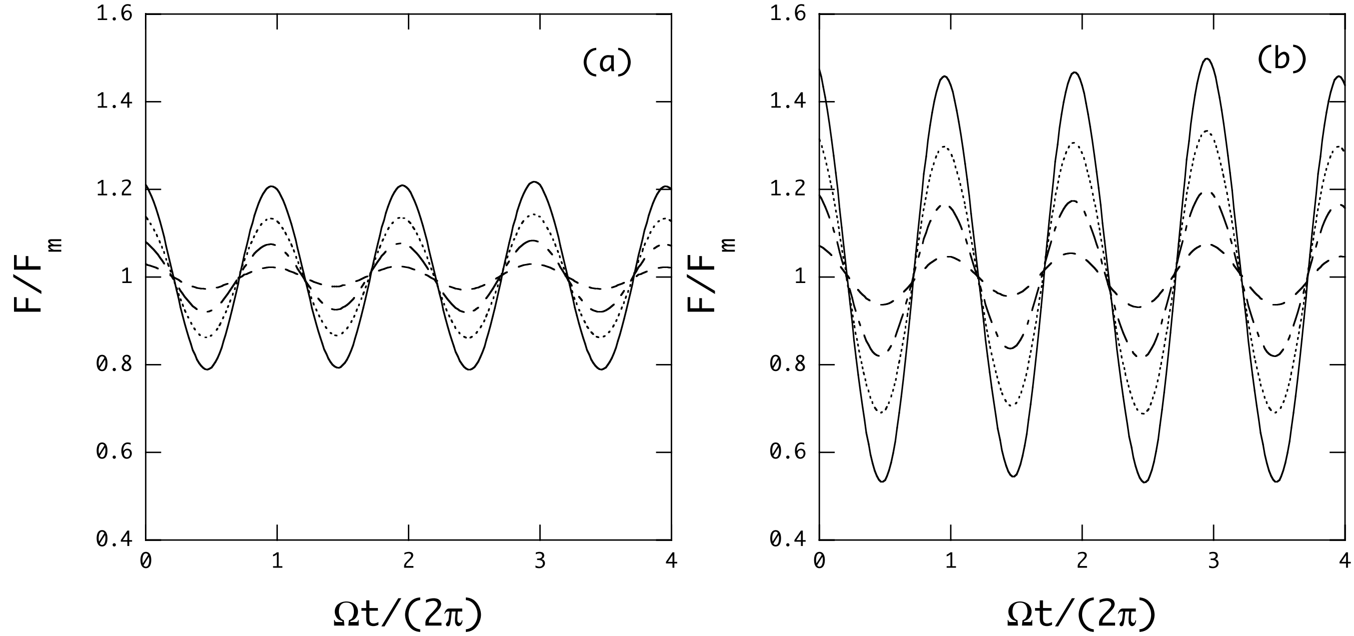

Figure 4. Light curves $F/F_{\rm m}$ produced by a hotspot of $\alpha = 20°$ for $\bar{\Omega} = 0.1$ as functions of $\Omega t/(2\pi)$ for $\theta_{\rm s} = 10°$ (panel a) and 30° (panel b), where $F_{\rm m}$ is the mean flux, and the dashed, dash–dotted, dotted and solid lines are for the inclination angles $i = 10°,\ 30°,\ 50°$ and 70°, respectively. Here, we assume $M = 1.4\,{\rm M}_\odot$ and $R = 10^6$ cm for the neutron star, and $\omega = 2\Omega/3$ and $A = 0.01$ for the $l' = m = 2$ r mode.

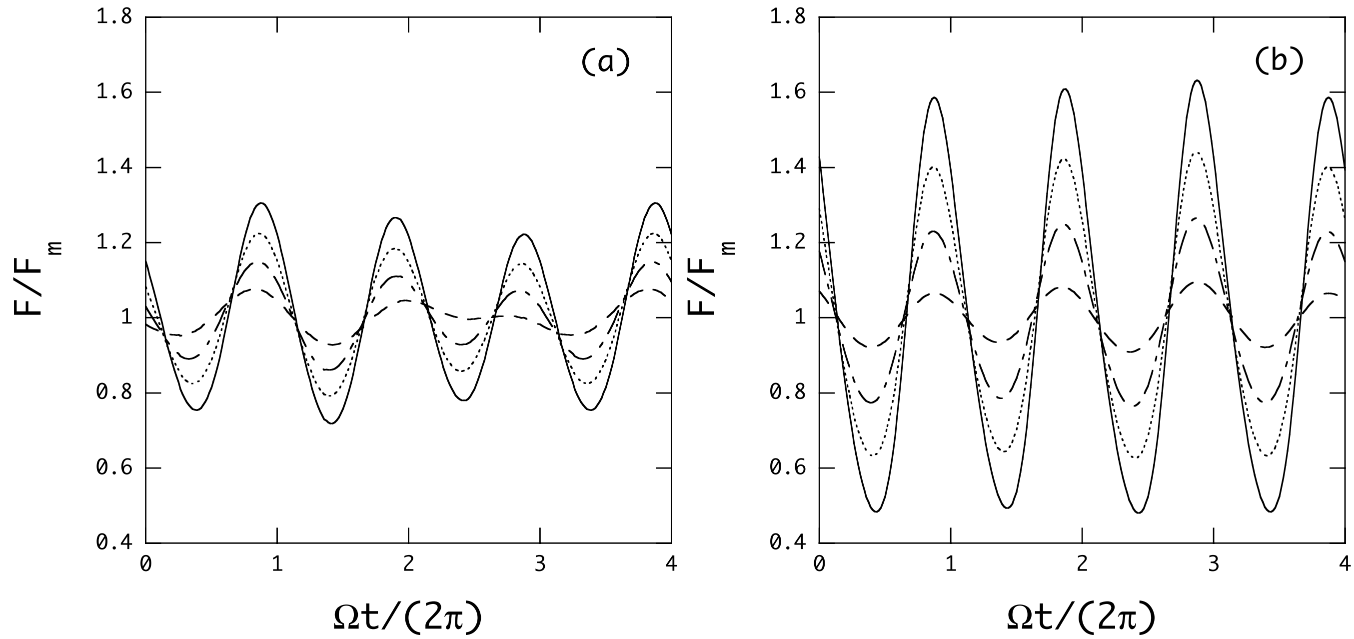

Figure 5. Same as Fig. 4, but for $\bar{\Omega} = 0.3$.

note that much weaker peaks, which seem to be proportional to the parameter A, are found at $\sigma_j = k\Omega \pm j2\Omega/3$ with k and j being integers as a result of non-linear couplings between the frequencies $k\Omega$ and $j2\Omega/3$.

The fractional amplitudes a_j/a_0 are plotted versus $\theta_{\rm s}$ in Fig. 7 for $\bar{\Omega} = 0.1$ and in Fig. 8 for $\bar{\Omega} = 0.3$. In general, the peaks at $\sigma_j = \Omega$ and 2Ω increase their height with increasing $\theta_{\rm s}$. On the other hand, the peak at $\sigma_j = 2\Omega/3$ shows rather a complicated behaviour with increasing $\theta_{\rm s}$, depending on the parameter α and the functions $\Xi_\theta(\hat{\theta})$ and $\Xi_\phi(\hat{\theta})$, but as $\theta_{\rm s} \to 0$ its height simply increases to become even higher than the peak at $\sigma_j = 2\Omega$, because in this limit the periodic deformation of the spot shape is the only cause for any periodicities. For the amplitude parameter $A = 10^{-3}$, for example, the amplitude a_j/a_0 at $\sigma_j = 2\Omega/3$ stays less than 10^{-3}, when $\theta_{\rm s} \gtrsim 10°$, for both cases of $\bar{\Omega} = 0.1$ and 0.3, but it becomes as large as ~0.01 for small values of $\theta_{\rm s}$. We also note that although the peaks at $\sigma_j = \Omega$ and 2Ω are dependent on the angle i, the peak at $\sigma_j = 2\Omega/3$ is almost insensitive to i, because no effects of the velocity field due to the r modes are included. Fig. 9 gives plots of

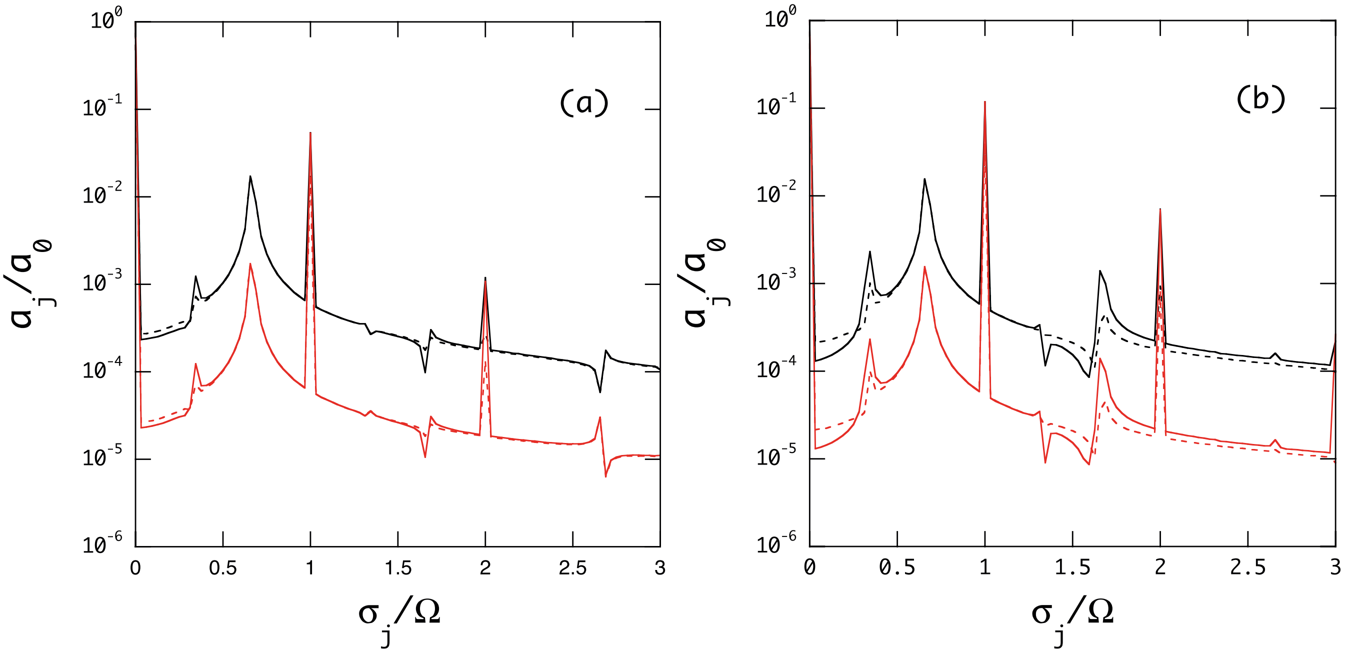

Figure 6. Normalized Fourier amplitudes a_j/a_0 as functions of σ_j/Ω calculated for light curves produced by a hotspot of $\alpha = 20^\circ$ for $\theta_s = 10^\circ$ (panel a) and 30° (panel b), where $\bar{\Omega} = 0.3$, and the black and red lines are for $A = 0.01$ and 0.001, respectively, and the solid and dotted lines are for the inclination angle $i = 30^\circ$ and 10°, respectively. Here, we assume $M = 1.4\,\mathrm{M}_\odot$ and $R = 10^6$ cm.

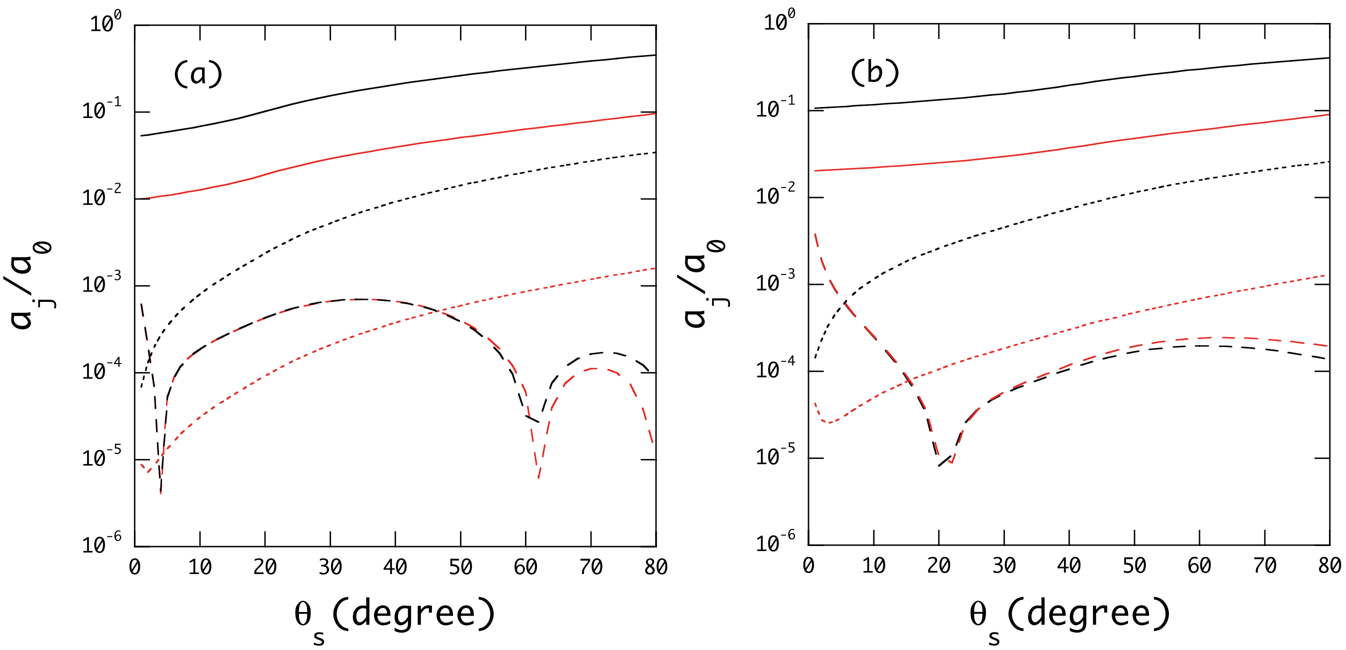

Figure 7. Normalized Fourier amplitudes a_j/a_0 as functions of the angular distance θ_s of the spot centre from the rotation axis of the star for $\alpha = 20^\circ$ (panel a) and $\alpha = 40^\circ$ (panel b), where the black and red lines are for $i = 50^\circ$ and 10°, respectively, and the solid, dotted and dashed lines are for the fundamental $\sigma_j = \Omega$, the first overtone $\sigma_j = 2\Omega$ and the $l' = m = 2$ r-mode $\sigma_j = 2\Omega/3$, respectively. Here, we assume $M = 1.4\,\mathrm{M}_\odot$, $R = 10^6$ cm and $\bar{\Omega} = 0.1$ for the neutron star and $A = 0.001$ for the mode.

$(X_\mathrm{b}, Y_\mathrm{b})$ and $(X_\mathrm{d}, Y_\mathrm{d})$ for the case of $\bar{\Omega} = 0.3$, $\alpha = 20^\circ$ and $\theta_s = 50^\circ$ corresponding to the deep dip found at $\theta_s = 50^\circ$ in the panel (a) of Fig. 8. We find that differences between the spot deformations in different phases Ωt are rather small compared to those found in the plots of $(X_\mathrm{b}, Y_\mathrm{b})$ and $(X_\mathrm{d}, Y_\mathrm{d})$ in Fig. 3, leading to the dip in a_j/a_0 associated with $\sigma_j = 2\Omega/3$. We have also examined the dependence of the amplitudes a_j/a_0 at $\sigma_j = 2\Omega/3$ on the compactness parameter r_g/R and found that the amplitudes are only weakly dependent on the parameter.

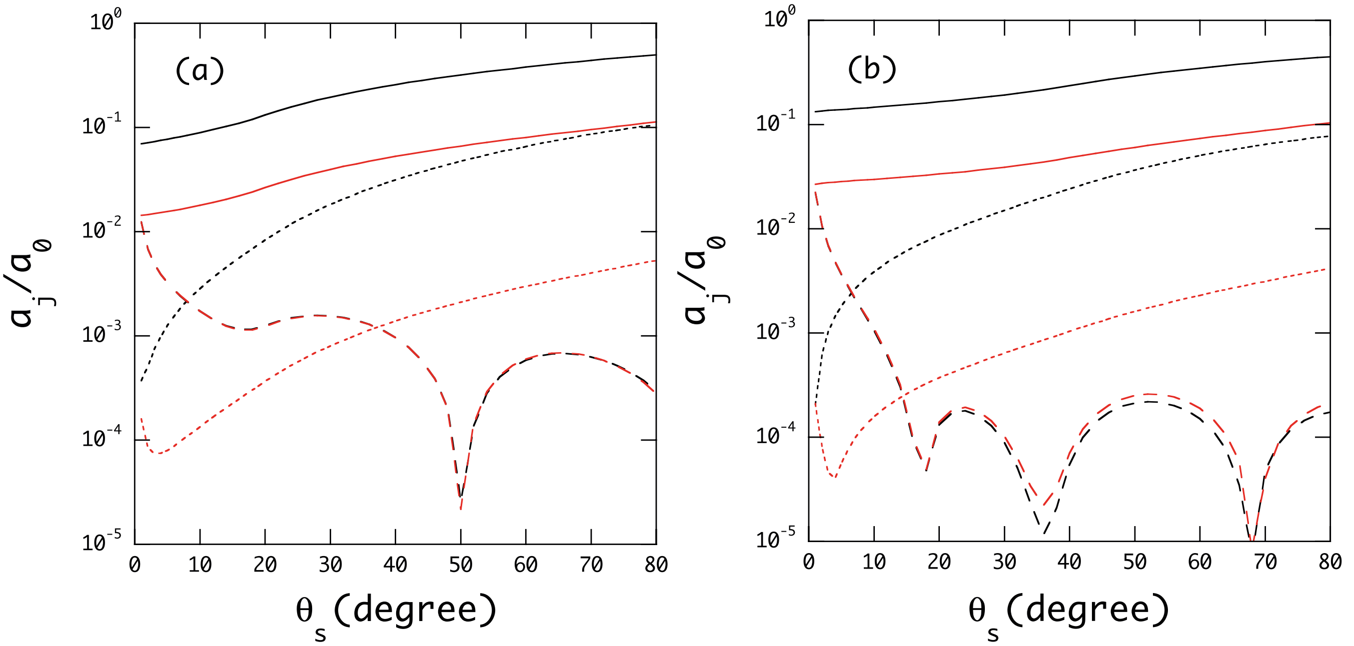

Figure 8. Same as Fig. 7, but for $\bar{\Omega} = 0.3$.

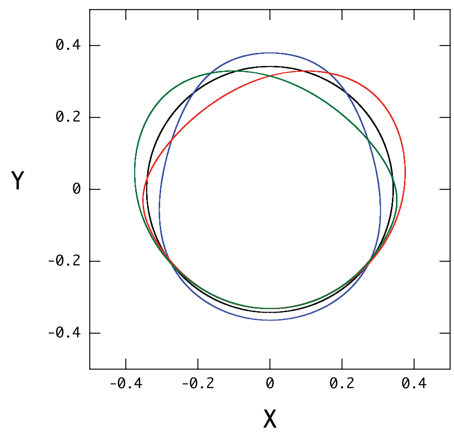

Figure 9. Plots of (X_b, Y_b) and (X_d, Y_d) for the spot of $\alpha = 20^\circ$ and $\theta_s = 50^\circ$, where we have used the functions Ξ_θ and Ξ_ϕ computed for the $l' = m = 2$ r mode at $\bar{\Omega} = 0.3$ and have assumed $\omega = 2\Omega/3$ and $A = 0.1$ for the plots. Here, the black curve is for the non-perturbed spot (X_b, Y_b) and the blue, red and green curves are for the perturbed spot (X_d, Y_d) for $\Omega t/(2\pi) = 0$, 1 and 2, respectively.

4 CONCLUSION

We have calculated light curves produced by a hotspot of a rapidly rotating neutron star, assuming that the hotspot is periodically disturbed by the horizontal displacement field of the $l' = m = 2$ core r mode, which is assumed to be excited by emitting gravitational waves. To calculate light curves, we have taken account of relativistic effects, such as the Doppler boost due to the rapid rotation and light bending, assuming the Schwarzschild metric around the star. We have also assumed that the oscillation frequency of the $l' = m = 2$ core r mode is exactly equal to $\omega = 2\Omega/3$ in the corotating frame of the star. It is found that a distant observer will detect in the light curves a periodicity due to the $l' = m = 2$ core r mode and that the observed frequency will be $2\Omega/3$, the frequency of the mode defined in the corotating frame of the star, instead of the frequency $4\Omega/3$ defined in an inertial frame for the mode. The fractional Fourier amplitude a_j/a_0 at $\sigma_j = 2\Omega/3$ in light curves is approximately proportional to the amplitude parameter A, which parametrizes the mode amplitude, such that $\max(|\Xi_\theta(\hat{\theta})|, |\Xi_\phi(\hat{\theta})|) = A$ for $0 \le \hat{\theta} \le \pi$. We find that besides the parameter A the amplitude a_j/a_0 at $\sigma_j = 2\Omega/3$ depends on the parameter θ_s, but it is almost insensitive to the parameters i and r_g/R. The reason for the insensitivity of a_j/a_0 to the parameters may be that no effects of the velocity field due to the r mode on light curves are taken into account in the calculations and the periodic deformation of the spot shape is restricted to a small area on the surface. For $A = 0.001$–0.01, the amplitude a_j/a_0 at $\sigma_j = 2\Omega/3$ will be ~ 0.001–0.01 and becomes comparable to or even greater than that of the first overtone at $\sigma_j = 2\Omega$, particularly for small values of θ_s.

If we write the oscillation frequency of the r modes observed in the corotating frame of the star as

$$\frac{\omega}{\Omega} = \kappa_0 + \kappa_2\bar{\Omega}^2 + O(\bar{\Omega}^4), \tag{28}$$

the coefficient κ_0 for the r modes with l' and m is simply given by

$$\kappa_0 = \frac{2m}{l'(l'+1)}, \tag{29}$$

and the coefficient κ_2 depends on the physical properties of neutron stars, such as the equation of state and the deviation from the isentropic stratification in the core (e.g. Yoshida & Lee 2000a,b). Since the neutron star core is nearly isentropic, such that $N^2 \sim 0$ with N being the Brunt–Väisälä frequency, we only have to consider the $l' = m$ r modes, for which we have $\omega \approx \kappa_0\Omega = 2\Omega/(m+1)$, and we obtain the frequency $\omega \approx 2\Omega/3$ for $m = 2$ in the corotating frame of the star. Although no detection of periodicities $\omega \approx 2\Omega/3$ associated with the $l' = m = 2$ core r mode has so far been reported, any detection of periodicities caused by the $l' = m$ core r modes in the X-ray millisecond pulsation makes it possible to use the frequency deviation given by $\Delta\bar{\omega} \equiv \bar{\omega} - \kappa_0\bar{\Omega} \approx \kappa_2\bar{\Omega}^3$ to derive information about the equations of state and the thermal stratification in the core.

Employing space–time metric numerically computed for rotating neutron stars instead of the Schwarzschild metric, Cadeau, Leahy & Morsink (2005) and Cadeau et al. (2007) have discussed the frame-dragging effects on the light curves produced by a small hotspot on the surface of rapidly rotating neutron stars. Cadeau et al. (2007) have concluded that in most cases, the differences in the light curves between the choices of metrics are smaller than the differences caused by the spherical or oblate shape of the initial emission surface. We think this is also the case for light curves produced by a finite hotspot periodically modified by the r mode. We may also guess that the effects of the rotational deformation of neutron stars on the frequency and surface wave pattern of the r mode, for example, could be more significant than the frame-dragging effects for light curves. We believe that at the current stage of investigation the frame dragging may be regarded as one of the effects that become discernible only after very accurate light-curve determination becomes possible observationally and theoretically.

To use a surface hotspot of a rapidly rotating neutron star as a probe into core r modes, the modes must penetrate the solid crust to have sufficient amplitudes at the surface. The detectability of periodicities due to the core r modes in light curves therefore may depend on, for example, the thickness of the solid crust, the property of the surface fluid ocean, the strength of the magnetic field, etc. In this paper, although we have used the functions Ξ_θ and Ξ_ϕ computed for a low-mass, cold neutron star model with a thick solid crust, which makes the frequency spectrum simple, it is desirable to use the functions computed for more massive neutron stars as well, which may have a thin solid crust and hence have a different oscillation frequency spectrum from that for a cold low-mass neutron star. For accretion-powered neutron stars, it is also desirable to use mass-accreting neutron star models with a hot fluid ocean and solid crust, with which we can examine how the amplitudes of core r modes at the surface depend on the physical properties of the fluid ocean and solid crust. The existence of a magnetic field is another important factor we have to consider, particularly to determine the wave patterns at the surface. Although the effects of a magnetic field on the displacement vector $\boldsymbol{\xi}$ of core r modes have been examined only for a dipole field, whose axis aligns with the spin axis, we need to examine how an oblique dipole field and a field different from a dipole one changes the surface wave patterns (e.g. Heng & Spitkovsky 2009).

Applying a weak non-linear theory, Arras et al. (2003) have estimated the saturation level for the r-mode energy $E_{\rm r-mode}$ by considering non-linear transfer of energy to the sea of stellar inertial oscillation modes of rotating stars with negligible buoyancy and elastic restoring force and without magnetic field. For the saturation energy in the strong driving limit of the r mode, they obtained an estimate given by $E_{\rm r\text{-}mode}/(0.5MR^2\Omega^2) \simeq 10^{-6}(\nu_{\rm spin}/10^3\,{\rm Hz})^5$, which may amount to the mode amplitude parameter $A \sim 10^{-3}(\nu_{\rm spin}/10^3\,{\rm Hz})^{5/2}$, where $\nu_{\rm spin}$ denotes the spin frequency of the star. If this amplitude estimation is correct, the amplitude parameter A for neutron stars spinning at $\nu_{\rm spin} \sim 500\,{\rm Hz}$ becomes of the order of 10^{-4}, which is one order of magnitude smaller than the value $A = 10^{-3}$ used in this paper for presentation and may suggest that the detectability of the periodic modulation due to the r modes is not very high even for small values of $\theta_{\rm s}$. In this paper, we have discussed the possibility of using X-ray light curves from a hotspot as a probe into the core r modes of neutron stars, but it is also conceivable that periodicities due to the r modes, which may shake the surface magnetic field, are contained in the pulses, possibly as drifting sub- or micro-pulses, from millisecond radio pulsars.

REFERENCES

Andersson N., 1998, ApJ, 502, 708
Arras P., Flanagan E. E., Morsink S. M., Schenk A. K., Teukolsky S. A., Wasserman I., 2003, ApJ, 591, 1129
Cadeau C., Leahy D., Morsink S. M., 2005, ApJ, 618, 451
Cadeau C., Morsink S. M., Leahy D., Campbell S. S., 2007, ApJ, 654, 458
Duncan R. C., 1998, ApJ, 498, L45
Friedman J. L., Morsink S. M., 1998, ApJ, 502, 714
Friedman J. L., Schutz B. F., 1978, ApJ, 222, 281
Ghisellini G., 2000, in Casciaro B., Fortunato D., Francaviglia M., Masiello A., eds, Recent Developments in General Relativity. Springer, Berlin, p. 5
Heng K., Spitkovsky A., 2009, ApJ, 703, 1819
Heyl J. S., 2004, ApJ, 600, 939
Heyl J. S., 2005, MNRAS, 361, 504
Israel G. et al., 2005, ApJ, 628, L53
Lamb F. K., Boutloukos S., 2008, in Milone E. F., Leahy D. A., Hobill D. W., eds, Astrophys. Space Sci. Libr. Vol. 352, Short-Period Binary Stars: Observations, Analyses, and Results. Springer, Berlin, p. 87

Lamb F. K., Boutloukos S., Van Wassenhove S., Chamberlain R. T., Lo K. H., Clare A., Yu W., Miller M. C., 2009, ApJ, 706, 417
Lee U., 2004, ApJ, 600, 914
Lee U., 2007, MNRAS, 374, 1015
Lee U., 2010, MNRAS, 405, 1444
Lee U., Strohmayer T. E., 2005, MNRAS, 361, 659
Lind K. R., Blandford R. D., 1985, ApJ, 295, 358
Lindblom L., Owen B. J., Morsink S. M., 1998, Phys. Rev. Lett., 80, 4843
Lockitch K. H., Friedman J. L., 1999, ApJ, 521, 764
McDermott P. N., Van Horn H. M., Hansen C. J., 1988, ApJ, 325, 725
Narayan R., Cooper R. L., 2007, ApJ, 665, 628
Owen B. J., Lindblom L., Cutler C., Schutz B. F., Vecchio A., Andersson N., 1998, Phys. Rev. D, 58, 084020
Pechenick K. R., Ftaclas C., Cohen J. M., 1983, ApJ, 274, 846
Poutanen J., Gierliński M., 2003, MNRAS, 343, 1301
Strohmayer T. E., Lee U., 1996, ApJ, 467, 773
Strohmayer T. E., Watts A. L., 2005, ApJ, 632, L111
Strohmayer T. E., Watts A. L., 2006, ApJ, 653, 593
Strohmayer T. E., Zhang W., Swank J. H., Smale A., Titarchuk L., Day C., Lee U., 1996, ApJ, 469, L9
Strohmayer T. E., Day C., Smale A. P., Swank J. H., Zhang W., Titarchuk L., Lee U., 1997, ApJ, 486, 355
Watts A. L., Strohmayer T. E., 2006, ApJ, 637, L117
Woods P. M., Thompson C., 2006, in Lewin W. H. G., van der Klis M., eds, Compact Stellar X-Ray Sources. Cambridge Univ. Press, Cambridge
Yoshida S., Lee U., 2000a, ApJ, 529, 997
Yoshida S., Lee U., 2000b, ApJS, 129, 353
Yoshida S., Lee U., 2001, ApJ, 546, 1121

This paper has been typeset from a TEX/LATEX file prepared by the author.